

Derivation of Equations Describing Distance Solute Oscillation of Induced Solvent Polarization

Pei-Kun Yang

Department of Biomedical Engineering, I-SHOU University, Kaohsiung 840, Taiwan

Received July 6, 2010; E-mail: peikun@isu.edu.tw

The dielectric polarization \mathbf{P} is the key factor for computing electromagnetic interactions between charged particles in materials in classical electrodynamics, and for computing hydration free energy of biomolecules in the field of physical chemistry. Near-solute \mathbf{P} dominates electric contributions to the solute from polarized solvent media and oscillates with decay according to the distance to the solute. This oscillating decay is observed in molecular dynamics simulations and cannot be reproduced from Gauss's law of Maxwell's equations. In the present paper, \mathbf{P} was decomposed into the electric dipole moment \mathbf{p} and the solvent density ρ . Equations and an approximate analytical solution capturing the oscillating decay of \mathbf{p} were derived for a spherical solute. The equations can be used to understand physically why \mathbf{p} oscillates according to the distance to the solute. The approximate analytical solution can identify factors, such as the solvent molecular radius R_W and the solvent molecular electric susceptibility χ_e^g , changing the amplitude and the oscillation period of \mathbf{p} . In addition, the approximate analytical solution of \mathbf{p} is similar to the solution of a spring system with harmonic damping. However, the equation describing \mathbf{p} uses a first-order integral equation and thus differs from the equation describing a spring system which uses a second-order differential equation.

Among the four fundamental types of interactions—strong, weak, gravitation, and electromagnetic—electromagnetic interactions dominate in molecular solutes, such as protein–protein/ligand/DNA interactions. Coulomb's law provides the means to calculate the electric interaction energy or force between two charged particles.^{1,2} Numerous polarized molecules exist in dielectric material, and to treat them as sources to evaluate electric interactions is almost impossible. Maxwell treats the electric effect of discrete polarized molecules as a space continuum distribution where the induced dielectric polarization $\mathbf{P}_{\text{Maxwell}}$ is the electric dipole moment averaged in a macroscopic region proportional to the electric field $\mathbf{E}_{\text{Maxwell}}$.^{1,2} $\mathbf{E}_{\text{Maxwell}}$ can be computed using the source charge and the induced $\mathbf{P}_{\text{Maxwell}}$. Both $\mathbf{P}_{\text{Maxwell}}$ and $\mathbf{E}_{\text{Maxwell}}$ can then be solved from these simultaneous equations by the given source charge.^{1,2}

The development of molecular biology^{3–5} and nanotechnology⁶ led to general concerns regarding the treatment of electric interactions among molecular solutes in solvent media. Water is the most abundant solvent on earth, without which life as we know it would not be possible.⁷ Electric interactions between two charged particles in water media are reduced compared with interactions in a vacuum environment, because water solvent molecules have large permanent dipole moments and can rotate. When r_{12} separates two charged particles in dielectric media with charged states Q_1 and Q_2 , then the components from particle 1 and from polarized solvent molecules can partition the electric force acting on particle 2. The first component is $\mathbf{F}_2^1 = Q_1 Q_2 \mathbf{r}_{12} / 4\pi\epsilon_0 r_{12}^3$, where ϵ_0 is the permittivity of free space and r_{12} is the vector from particle 1 to particle 2.^{1,2} To compute the second component \mathbf{F}_2^P , the induced solvent dielectric polarization \mathbf{P} has to be estimated.

Gauss's law of Maxwell's equations, $\nabla \cdot \mathbf{D} = \rho$,^{1,2} provides an approximate way to estimate \mathbf{P} . For a charged particle with the charged state Q_1 immersed in material with a dielectric constant ϵ_r , \mathbf{P} is $\mathbf{P}_{\text{Maxwell}} = Q_1(1 - 1/\epsilon_r)\mathbf{r}/4\pi r^3$, where r is the distance to particle 1. Thus, the second component is $\mathbf{F}_2^{P, \text{Maxwell}} = -Q_1 Q_2(1 - 1/\epsilon_r)\mathbf{r}_{12}/4\pi\epsilon_0 r_{12}^3$. The net force on particle 2 is then $\mathbf{F}_2 = Q_1 Q_2 \mathbf{r}_{12}/4\pi\epsilon_0 \epsilon_r r_{12}^3$, which is the sum of \mathbf{F}_2^1 and $\mathbf{F}_2^{P, \text{Maxwell}}$.^{1,2}

Taking a water solvent with a dielectric constant $\epsilon_r = 80$ as an example, the second component cancels 79/80 of the force from the first component, leaving only 1/80 of the force from particle 1 and 2/80 with a 1% computing error for \mathbf{F}_2^P . The computing error doubles the \mathbf{F}_2 error. Therefore, it is crucial to estimate the induced dielectric polarization \mathbf{P} accurately for computing electric interactions between two charged particles in water.

\mathbf{P} is useful for computing electric interactions between two charged particles in dielectric material, magnetic interactions,^{1,2} and the charging hydration free energy of a solute.^{8–12} For magnetic interactions, Ampere's law of Maxwell's equations, $\nabla \times \mathbf{H} = \mathbf{J} + \partial(\epsilon_0 \mathbf{E} + \mathbf{P})/\partial t$, determines the relation between the magnetic field and the time-dependent dielectric polarization \mathbf{P} .^{1,2} The \mathbf{P} is a major component to estimate the protein–protein/ligand binding affinity, which is useful for protein function studies^{4,7} and computer-aided drug design.^{13–15} In 1920, Born¹⁶ derived the charging hydration free energy $\Delta G_{\text{solv}}^{\text{elec}}$ by charging up $\Phi(q)$, the electrostatic potential at a solute due to the polarized solvent molecules, i.e., $\Delta G_{\text{solv}}^{\text{elec}} = \int_0^Q \Phi(q) dq$. $\Phi(q)$ was estimated considering a spherical ion of radius R_{Born} and charge Q immersed in a solvent with a dielectric constant ϵ_r . The ion polarizes the solvent and generates an induced dielectric polarization

$P_{\text{Maxwell}} = Q(1 - 1/\epsilon_r)r/4\pi r^3$, which contributes $-q(1 - 1/\epsilon_r)/(4\pi\epsilon_0 R_{\text{Born}})$ to the electrostatic potential at the ion with radius R_{Born} . The free energy obtained from the transfer of an ion from vacuum to a medium is $\Delta G_{\text{Born}} = -166Q^2(1 - 1/\epsilon_r)/R_{\text{Born}}$.

The induced solvent dielectric polarization effect significantly affects in numerous applications, such as computing electric interactions between charged particles in dielectric material, magnetic field, and charging hydration free energy of solute. Therefore, several methods including molecular dynamics (MD) simulations,^{17,18} Monte Carlo simulations,^{19–21} integral equations,^{22–26} and continuum dielectric methods^{9,11,27} were developed to compute the induced solvent dielectric polarization effect. Gauss's law of Maxwell's equations is the conventional way to compute the induced solvent dielectric polarization \mathbf{P} , which is then used to calculate the electric field contributed from polarized solvents or the charging hydration free energy.¹⁰ One of the advantages of Gauss's law of Maxwell's equations is that it provides analytical solutions for special cases and that it provides a physical sense to understand factors affecting the induced solvent dielectric polarization \mathbf{P} and thus the charging hydration free energy.^{1,2} The induced solvent dielectric polarization \mathbf{P} , defined as the average dipole moment over a microscopic region for a period of time, has a large peak in the near solute region and oscillates with decay depending on the distance to the solute observed in MD simulations. Gauss's law of Maxwell's equation, P_{Maxwell} , cannot obtain such an oscillation (Figure 1).²⁸ Although the structural solvent can be observed in MD simulations,^{28–30} they cannot provide a physical sense of the structural solvent. The near-solute \mathbf{P} contributes a significant electric effect to the solute. Therefore, the description of P_{Maxwell} in Gauss's law of Maxwell's equations, fails to capture the oscillating decay and cannot estimate the electric effect on nearby solutes. Although Gauss's law of Maxwell's equations can treat electric interactions between macroscopic objects, it is not suitable for molecular solutes with nanometer dimensions. An equation, which could reproduce oscillating decay characteristics and an analytical solution for spherical solutes, could examine why the oscillating decay of \mathbf{P} depends on the distance to the solute and what factors affect the oscillating decay of \mathbf{P} .

The present paper decomposes the solvent dielectric polarization $\mathbf{P}(\mathbf{r})$ into microscopic solvent densities $\rho(\mathbf{r})$ (the number of solvent molecules per unit volume over a time period in a microscopic region), and into electric dipole moments $\mathbf{p}(\mathbf{r})$ (the electric dipole moment of the solvent molecules averaged over a time period in a microscopic region). An approximate equation is derived for a spherical solute using $\mathbf{p}(\mathbf{r})$, because $\mathbf{p}(\mathbf{r})$ is the key factor in generating the distance solute oscillation decay of $\mathbf{P}(\mathbf{r})$ ²⁸ (Figure 2). Furthermore, an approximate analytical solution of $\mathbf{p}(\mathbf{r})$ is proposed and verified using MD simulations.

Theory

Qualitative Basis for the Oscillation of \mathbf{P} . Considering only solvent molecules in the region between $R - R_c$ and $R + R_c$, Coulomb's law can be used to evaluate the electric field acting on solvent molecules at R due to other solvent molecules (Figure 1). R_{max} and R_{min} denote the first peak

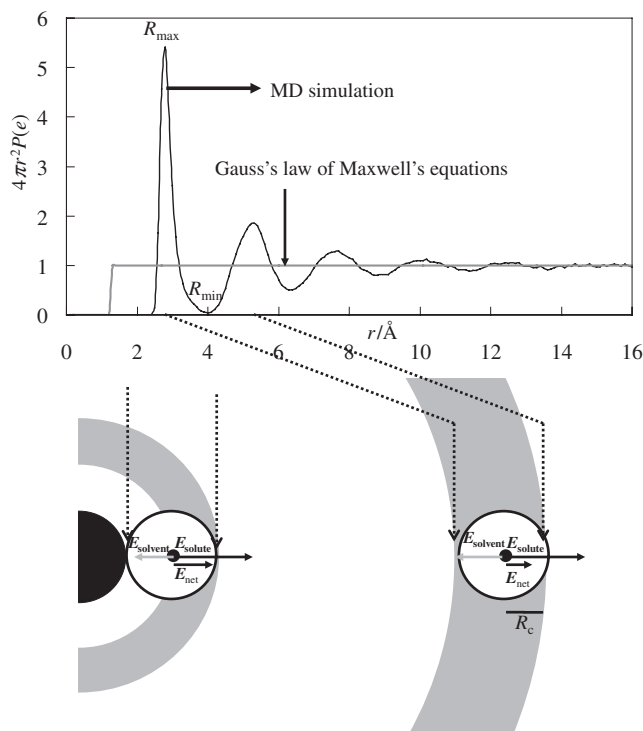


Figure 1. Comparison of $\mathbf{P}(\mathbf{r})$ from MD simulations and Gauss's law of Maxwell's equations. The $\mathbf{P}(\mathbf{r})$ as a function of distance r from a charged solute atom with the charge state $Q = 1e$ was computed from MD simulations (black curve)^{28,31} and macroscopic Gauss's law of Maxwell's equations (gray curve). The $\mathbf{P}(\mathbf{r})$ from MD simulation decays in an oscillatory manner away from the solute (top panel). The solvent dielectric polarization at a distance r from the solute depends on the net electric field $E_{\text{net}}(\mathbf{r})$ acting on the solvent molecule at r , which can be decomposed into contributions from the solute $E_{\text{solute}}(\mathbf{r})$ and the other solvent molecules $E_{\text{solvent}}(\mathbf{r})$. Only those solvent molecules in the annular region between $r - R_c$ and $r + R_c$ contribute to $E_{\text{solvent}}(\mathbf{r})$, while the other solvent molecules do not contribute to $E_{\text{solvent}}(\mathbf{r})$ on the basis of Gauss's law (bottom panel).

position and the first valley position of the solvent dielectric polarization \mathbf{P} (Figure 1). Few solvent molecules exist in the region within R_{max} of the solute, thus the electric field E_{solvent} caused by solvent molecules in the region " $R_{\text{max}} - R_c$ to $R_{\text{max}} + R_c$ " cannot offset the electric field E_{solute} caused by the solute. However, the electric field E_{solvent} almost offsets the electric field E_{solute} , because the solvent dielectric polarization \mathbf{P} in the region " $R_{\text{min}} - R_c$ to $R_{\text{min}} + R_c$ " is larger than \mathbf{P} in the bulk solvent region. Consequently, the net electric field E_{net} is far greater at R_{max} than at R_{min} , which attracts more solvent molecules to the annular region at R_{max} . This enhances the solvent density ρ , the electric dipole moment \mathbf{p} , and thus the solvent dielectric polarization \mathbf{P} at R_{max} relative to R_{min} .

Introduction of Equations Reproducing the Near-Solute Oscillation of the Induced Solvent Dielectric Polarization \mathbf{P} . Solute molecules immersed in solvent media exclude and polarize surrounding solvent molecules and perturb the surrounding solute solvent density ρ and electric dipole

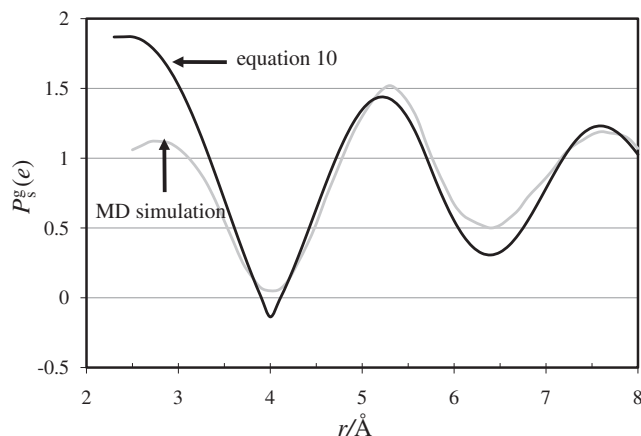


Figure 2. Comparison of $P_s^g(r)$ from eq 10 and MD simulations. $P_s^g(r)$ as a function of distance r from charged solute atom was computed from eq 10 with numerical strategy (black curve) and MD simulations (gray curve).^{28,31} In eq 10, the solute charge state $Q = 1e$, the solute molecular radius $R_{\text{solute}} = 2.3 \text{ Å}$, the solvent molecular radius $R_W = 1.7 \text{ Å}$, and the solvent molecular electric susceptibility $\chi_c^g = 4.4$.

moment \mathbf{p} . Previous studies computed the solvent density $\rho(r)$ and electric dipole moment $\mathbf{p}(r)$ from a given solute charge Q , the solute/solvent size, intermediated by the force $\mathbf{F}(r)$, and the electric field $\mathbf{E}(r)$ on the solvent molecule.^{28,31} The following introduces equations calculating the distance solute oscillation of the induced electric dipole moment $\mathbf{p}(r)$.

To describe the distance solute oscillation of \mathbf{P} , $\mathbf{P}(r)$ is decomposed into $g(r)$, the solvent molecular density distribution (defined as the ratio between the solvent density ρ and the bulk solvent density N_{bulk}), N_{bulk} , the bulk solvent density, and $\mathbf{p}(r)$, the electric dipole moment, i.e.,

$$\mathbf{P}(r) = N_{\text{bulk}} g(r) \mathbf{p}(r) \quad (1)$$

For a perfect dipole moment at the center of the van der Waals (vdW) sphere, the electric dipole moment $\mathbf{p}(r)$ in eq 1 is approximately proportional to the electric field $\mathbf{E}(r)$

$$\mathbf{p}(r) = \varepsilon_0 \gamma_{\text{mol}} \mathbf{E}(r) \quad (2)$$

where ε_0 is the permittivity of vacuum and γ_{mol} is the solvent molecular polarizability.^{2,28}

The electric field $\mathbf{E}(r)$ of a solvent molecule at \mathbf{r} can be computed from a solute with a charge distribution $\rho_{\text{solute}}(\mathbf{r}')$ and from other solvent molecules with the induced solvent dielectric polarization $\mathbf{P}(\mathbf{r}, \mathbf{r}')$ perturbed by the solvent molecule at \mathbf{r} .

$$\mathbf{E}(r) = - \int [\rho_{\text{solute}}(\mathbf{r}') - \nabla' \cdot \mathbf{P}(\mathbf{r}, \mathbf{r}')] \nabla (1/4\pi\varepsilon_0 |\mathbf{r} - \mathbf{r}'|) d^3 \mathbf{r}' \quad (3)$$

where $\mathbf{P}(\mathbf{r}, \mathbf{r}')$ is the solvent dielectric polarization at \mathbf{r}' , when one of the solvent molecules is at \mathbf{r} .

The continuum-type approximation simplifies the estimation of $\mathbf{P}(\mathbf{r}, \mathbf{r}')$. The solvent molecule at \mathbf{r} perturbing other solvent molecules is treated as a spherical cavity with a radius R_W . Within the region occupied by the solvent molecule at \mathbf{r} with radius R_W , $\mathbf{P}(\mathbf{r}, \mathbf{r}')$ is approximately zero and is

$$\mathbf{P}(\mathbf{r}, \mathbf{r}') = \mathbf{P}(\mathbf{r}') u(|\mathbf{r} - \mathbf{r}'| - R_W) \quad (4)$$

Where $u(|\mathbf{r} - \mathbf{r}'| - R_W)$ is the Heaviside unit step function.

Derivation of Equation $P_s^g(r)$ for the Spherical Solute.

Although the simultaneous equations can find a numerical solution for $\mathbf{P}(r)$, $\mathbf{p}(r)$, and $g(r)$,²⁸ an analytical solution may explore the oscillating decay (affected by the distance to the solute) characteristic of $\mathbf{p}(r)$ in a physical sense (Figure 2).^{28,31} For a solute composed of n atoms, it is difficult to find an analytical solution of $\mathbf{P}(r)$ and $\mathbf{p}(r)$, because an analytical solution of $\mathbf{P}_{\text{Maxwell}}(r)$ cannot be found. Hence, a spherical charged solute with a charged state Q is assumed here due to the spherical symmetry of $\mathbf{P}(r)$ and $\mathbf{p}(r)$. The electric field $\mathbf{E}(r)$ generated from the induced solvent dielectric polarization $\mathbf{P}(\mathbf{r}')$ outside the region $r' < (r - R_W)$ and $r' > (r + R_W)$ is zero in eq 3 due to Coulomb's law.^{1,2} Only $\mathbf{P}(\mathbf{r}')$ in the region $(r - R_W)$ and $(r + R_W)$ and the solute charge Q contribute to the electric field $\mathbf{E}(r)$ of the solvent molecule at \mathbf{r} , where R_W is the radius occupied by the solvent molecule. Hence, the electric field $\mathbf{E}(r)$ along a radial direction is³²

$$E(r) = \frac{Q}{4\pi\varepsilon_0 r^2} - \frac{1}{4\varepsilon_0 R_W r^2} \int_{r-R_W}^{r+R_W} P(r')(r^2 + r'^2 - R_W^2) dr' \quad (5)$$

Using eq 2, $p(r)$ replaces $E(r)$ and $g(r')$ and $p(r')$ replace $P(r')$ using eq 1. Thus, the relationship between $p(r)$, $g(r')$ and Q becomes

$$p(r) = \frac{\gamma_{\text{mol}} Q}{4\pi r^2} - \frac{\chi_c^g}{4R_W r^2} \int_{r-R_W}^{r+R_W} g(r') p(r')(r^2 + r'^2 - R_W^2) dr' \quad (6)$$

where $\chi_c^g \equiv N_{\text{bulk}} \gamma_{\text{mol}}$. Based on Gauss's law of Maxwell's equations, $p(r)$ should be proportional to $1/r^2$ in the far solute region. Therefore, $P_s^g(r)$ is

$$P_s^g(r) \equiv \frac{4\pi r^2 P(r)}{g(r)} = 4\pi r^2 N_{\text{bulk}} p(r) \quad (7)$$

After $P_s^g(r)$ in eq 7 replaces $p(r)$ in eq 6, eq 6 changes to

$$P_s^g(r) + \frac{\chi_c^g}{4R_W} \int_{r-R_W}^{r+R_W} g(r') P_s^g(r') \left(1 + \frac{r^2 - R_W^2}{r'^2}\right) dr' = \chi_c^g Q \quad (8)$$

Equation 8 describes the relationship between $P_s^g(r)$ and the solute charge Q and contains the unknown variable $g(r)$. The simplest way to mimic characteristics of $g(r)$ is to use a continuum-type approximation assuming a Heaviside unit step function $-u(r - R_{\text{solute}})$, where $g(r)$ is zero in the solute occupied region and a bulk solvent outside the solute occupied region. To be more specific, $g(r) = 0$ if $r < R_{\text{solute}}$ and $g(r) = 1$ if $r > R_{\text{solute}}$, where R_{solute} is the radius of the cavity excluding solvent molecules. Then eq 8 becomes

$$P_s^g(r) + \frac{\chi_c^g}{4R_W} \int_{\text{Max}(R_{\text{solute}}, r-R_W)}^{r+R_W} P_s^g(r') \left(1 + \frac{r^2 - R_W^2}{r'^2}\right) dr' = \chi_c^g Q \quad (9)$$

where $\text{Max}(R_{\text{solute}}, r - R_W)$ is the maximum value of R_{solute} or $(r - R_W)$. $P_s^g(r)$ can be calculated using a given solute charge Q and the size of the solute R_W in eq 9. To capture oscillating decay characteristics of $P_s^g(r)$, eq 9 is simplified assuming

$r' \approx r$ and $R_W \ll r$. Then the relation between $P_s^g(r)$ and Q can be approximated as

$$P_s^g(r) + \frac{\chi_c^g}{2R_W} \int_{\text{Max}(R_{\text{solute}}, r-R_W)}^{r+R_W} P_s^g(r') dr' = \chi_c^g Q \quad (10a)$$

Equation 10a is the integral form of $P_s^g(r)$, which can be converted into the differential form

$$\frac{dP_s^g(r)}{dr} = \begin{cases} -\frac{\chi_c^g}{2R_W} [P_s^g(r+R_W) - P_s^g(r-R_W)] & r \geq R_{\text{solute}} + R_W \\ -\frac{\chi_c^g}{2R_W} P_s^g(r+R_W) & R_{\text{solute}} < r < R_{\text{solute}} + R_W \end{cases} \quad (10b)$$

Derivation of the Approximate Analytical Solution of $P_s^g(r)$ for the Spherical Solute. To obtain an approximate analytical solution of $P_s^g(r)$, characteristics of $P_s^g(r)$ in eq 10 were analyzed.

The Solution of $P_s^g(r)$ in eq 10 Oscillates: In the region $r > R_{\text{solute}} + R_W$, $dP_s^g(r_0)/dr > 0$ at the position $r = r_0$. If $dP_s^g(r)/dr > 0$ in the region $(r_0 - R_W) \leq r \leq (r_0 + R_W)$, then $P_s^g(r_0 + R_W)$ should be greater than $P_s^g(r_0 - R_W)$. By incorporating the inequality $P_s^g(r_0 + R_W) > P_s^g(r_0 - R_W)$ into the right side of eq 10b, $dP_s^g(r_0)/dr$ should be smaller than zero. However, this would violate the assumption that $dP_s^g(r)/dr > 0$ in the region $(r_0 - R_W) \leq r \leq (r_0 + R_W)$. Hence, $dP_s^g(r_0)/dr$ cannot always be greater than zero in the region $(r_0 - R_W) \leq r \leq (r_0 + R_W)$. This may indicate that $dP_s^g(r_1)/dr < 0$ at a position r_1 in the region $(r_0 - R_W) \leq r_1 \leq (r_0 + R_W)$. Thus, $(dP_s^g(r_0)/dr \times dP_s^g(r_1)/dr) < 0$ can be found at the two positions r_0 and r_1 in the region $(r - R_W)$ and $(r + R_W)$. The sign of the slope $dP_s^g(r)/dr$ changes in the region $(r - R_W)$ and $(r + R_W)$ for $r > (R_{\text{solute}} + R_W)$. The mean curve of $P_s^g(r)$ should oscillate with a period less than or equal to $2R_W$ according to the distance to the solute.

Dependence of the Amplitude and Period of $P_s^g(r)$ on the Solute Charge Q and the Solvent Molecular Radius R_W : Replacing the solute charge Q by cQ , where c is a constant, can reveal the relationship between the amplitude of $P_s^g(r)$ and the solute charge Q . If $P_s^g(r)$ was the solution of eq 10a with the solute charge state Q , and $P_s^g(r)$ was the solution of eq 10a with the solute charge state cQ , then $P_s^g(r) + \chi_c^g/(2R_W) \int_{\text{Max}(R_{\text{solute}}, r-R_W)}^{r+R_W} P_s^g(r') dr' = \chi_c^g cQ$. The solution for $P_s^g(r)$ is estimated as $P_s^g(r) = cP_s^g(r)$. Replacing the estimated solution leads to $cP_s^g(r) + c\chi_c^g/(2R_W) \int_{\text{Max}(R_{\text{solute}}, r-R_W)}^{r+R_W} P_s^g(r') dr' = \chi_c^g cQ$. Dividing the above equation by the constant c on both sides, reveals that $P_s^g(r) = cP_s^g(r)$ is the solution when the solute charge is cQ . This demonstrates that the solution of $P_s^g(r)$ in eq 10 is proportional to the solute charge Q .

Replacing the cavity radius occupied by the solvent molecule R_W with cR_W , where c is a constant, can examine the relationship between $P_s^g(r)$ and the solvent molecular radius R_W . If $P_s^g(r)$ was the solution of eq 10a with the cavity radius occupied by the solvent molecule R_W , and if $P_s^g(r)$ was the solution of eq 10a with the cavity radius occupied by the solvent molecule cR_W , then $P_s^g(r) + \chi_c^g/(2cR_W) \int_{r-cR_W}^{r+cR_W} P_s^g(r') dr' = \chi_c^g cQ$. Setting $r'' = r'/c$, changes the above equation $P_s^g(r) + \chi_c^g/$

$(2R_W) \int_{r/c-R_W}^{r/c+R_W} P_s^g(r'') dr'' = \chi_c^g Q$. The solution for $P_s^g(r)$ is $P_s^g(r/c)$, implying that the oscillation period of $P_s^g(r)$ in eq 10 is proportional to the cavity radius occupied by the solvent molecule R_W .

Analytical Solution in the Region $r \geq (R_{\text{solute}} + R_W)$: The solution for $P_s^g(r)$ in eq 10 can consist of a particular solution y_p and a homogeneous solution y_h as $P_s^g(r) = y_p(r) + y_h(r)$. For a particular solution, $y_p(r)$ is estimated as a constant. Then $y_p(r)$ have to satisfy the following condition:

$$y_p(r) + \frac{\chi_c^g}{2R_W} \int_{r-R_W}^{r+R_W} y_p(r') dr' = \chi_c^g Q \quad r \geq R_{\text{solute}} + R_W \quad (11)$$

Thus, $y_p(r) = \chi_c^g Q / (1 + \chi_c^g)$.

A homogeneous solution $y_h(r)$ should satisfy the differential equation

$$\frac{dy_h(r)}{dr} = -\frac{\chi_c^g}{2R_W} [y_h(r+R_W) - y_h(r-R_W)] \quad r \geq R_{\text{solute}} + R_W \quad (12)$$

The solution for $y_h(r)$ should oscillate. Hence, the homogeneous solution $y_h(r)$ is an oscillation decay function

$$y_h(r) = Ce^{-A(r-R_{\text{solute}}-R_W)} \cos(B(r-R_{\text{solute}}-R_W)) \quad r \geq R_{\text{solute}} + R_W \quad (13)$$

The coefficients A , B , and C are constants. A is greater than zero because the oscillation peak $P_s^g(r)$ observed in MD simulations decays according to the distance to the solute. B is assumed greater than zero because the cosine function is an even function. Due to the above analysis, B should be inversely proportional to the solvent molecular radius R_W and C should be proportional to the solute charge state Q . Inserting the solution for $y_h(r)$ from eq 13 into eq 12, can compute the coefficients A and B (see Appendix I).

$$\begin{cases} A = -\frac{\chi_c^g}{R_W} \sinh(AR_W) \cos(BR_W) \\ B = -\frac{\chi_c^g}{R_W} \cosh(AR_W) \sin(BR_W) \end{cases} \quad (14a)$$

Furthermore, if $A' = AR_W$ and $B' = BR_W$, then eq 14a could be rewritten as

$$\begin{cases} A' = -\chi_c^g \sinh A' \cos B' \\ B' = -\chi_c^g \cosh A' \sin B' \end{cases} \quad (14b)$$

Given the solvent molecular electric susceptibility χ_c^g , eq 14b can solve A' and B' , which in turn can be used to compute the coefficients A and B .

Hence, the proposed analytical solution is

$$P_s^g(r) = \frac{\chi_c^g Q}{1 + \chi_c^g} + Ce^{-A(r-R_{\text{solute}}-R_W)} \cos(B(r-R_{\text{solute}}-R_W)) \quad r \geq R_{\text{solute}} + R_W \quad (15)$$

The Analytical Solution in the Region $R_{\text{solute}} < r \leq R_{\text{solute}} + R_W$: In this region, $dP_s^g(r)/dr$ satisfies the conditions in eq 10b. After inserting the solution for $P_s^g(r)$ from eq 15 into the right side of eq 10b, the integration of $P_s^g(r)$ over r (see Appendix II) can solve $P_s^g(r)$ in the region $R_{\text{solute}} < r \leq R_{\text{solute}} + R_W$ as follows:

$$\begin{aligned}
P_s^g(r) = & \frac{\chi_c^g Q}{1 + \chi_c^g} + C \\
& + C \frac{\chi_c^g}{2R_W} \frac{e^{-AR_W}}{A^2 + B^2} [B \sin(BR_W) - A \cos(BR_W)] \\
& - \frac{\chi_c^g}{2R_W} \frac{\chi_c^g Q}{1 + \chi_c^g} (r - R_{\text{solute}} - R_W) \\
& - C \frac{\chi_c^g}{2R_W} \frac{e^{-A(r-R_{\text{solute}})}}{A^2 + B^2} [B \sin(B(r - R_{\text{solute}})) \\
& - A \cos(B(r - R_{\text{solute}}))] \quad (16a)
\end{aligned}$$

Equation 16a can be simplified with an approximate strategy. If $(A^2 + B^2)$ were far greater than 1.0 (Figure 3), then

$$P_s^g(r) = \begin{cases} \frac{\chi_c^g Q}{1 + \chi_c^g} \left[1 - \frac{(\chi_c^g)^2}{4(2 + \chi_c^g)} e^{-A(r-R_{\text{solute}}-R_W)} \cos(B(r - R_{\text{solute}} - R_W)) \right] & r \geq R_{\text{solute}} + R_W \\ \frac{\chi_c^g Q}{1 + \chi_c^g} \left[1 - \frac{(\chi_c^g)^2}{4(2 + \chi_c^g)} - \frac{\chi_c^g}{2R_W} (r - R_{\text{solute}} - R_W) \right] & R_{\text{solute}} < r \leq R_{\text{solute}} + R_W \end{cases} \quad (17)$$

The Oscillation Period of $P_s^g(r)$: The oscillation period of $P_s^g(r)$ can be calculated differentiating $P_s^g(r)$ in the region $r \geq (R_{\text{solute}} + R_W)$, and finding the position $r = R_{\text{solute}} + R_W + [\pi - \tan^{-1}(A/B)]/B$, where $dP_s^g(r)/dr = 0$ (see Appendix IV). Therefore, the period of $P_s^g(r)$ in the region $r \geq (R_{\text{solute}} + R_W)$ is $2\pi/B$.

Calculations

The Numerical Strategy Used to Estimate the Solution for $P_s^g(r)$ from eq 10. Given the cavity radius occupied by the solvent molecule R_W , the solvent molecular electric susceptibility χ_c^g , the solute charge state Q , and the solute molecular radius R_{solute} , an iterative numerical strategy can calculate $P_s^g(r)$. An adequate initial value of $P_s^g(0, r)$, the value of $P_s^g(r)$ in the 0th step, can converge the result more quickly. Applying Gauss's law of Maxwell's equations can estimate the initial value of $P_s^g(0, r)$. In the region $r < R_{\text{solute}}$, $P_s^g(0, r)$ is zero due to the absence of solvent molecules in the solute occupied region. In the region $r > R_{\text{solute}}$, $P_s^g(0, r) = \chi_c^g Q / (1 + \chi_c^g)$.

To understand whether $P_s^g(0, r)$ should increase or decrease in the region $r \geq R_{\text{solute}}$, the judgment function $J(r)$ is defined as, $J(r) = P_s^g(r) + \chi_c^g / (2R_W) \int_{\text{Max}(R_{\text{solute}}, r-R_W)}^{r+R_W} P_s^g(r') dr' - \chi_c^g Q$. Given the values of χ_c^g , R_W , Q , and R_{solute} , the judgment function $J(r)$ is calculated for each point in the region $R_{\text{solute}} \leq r \leq 20 \text{ \AA}$ step 0.01 \AA , by inserting $P_s^g(r)$ into the right side of the above equation. If $r = r_0$, and $J(r_0) < 0$, then $P_s^g(r_0) = P_s^g(r_0) + \Delta$, otherwise $P_s^g(r_0) = P_s^g(r_0) - \Delta$. The increasing number Δ is 0.0001. The iterations continue until all the points in the region $R_{\text{solute}} \leq r_0 \leq 20 \text{ \AA}$ result in an absolute value of $J(r) < 0.01$.

The Numerical Strategy to Solve the Coefficients A' and B' in eq 14b. To solve $P_s^g(r)$ from eq 17, A and B , which are dependent on the parameters χ_c^g and R_W , have to be known in the region $r \geq (R_{\text{solute}} + R_W)$. Both A and B can be computed from A' and B' , and A' and B' can be computed from χ_c^g using eq 14b. Thus, a given χ_c^g can provide a solution for A' and B' .

To judge whether the estimated sets (A', B') satisfy eq 14b, the judgment functions $J_1(A', B')$ and $J_2(A', B')$ were defined as $J_1 = A' + \chi_c^g \sinh A' \cos B'$ and $J_2 = B' + \chi_c^g \cosh A' \sin B'$,

the $1/(A^2 + B^2)$ component in eq 16a could be neglected. Thus, $P_s^g(r)$ in eq 16a can be simplified as

$$P_s^g(r) \approx \frac{\chi_c^g Q}{1 + \chi_c^g} + C - \frac{\chi_c^g}{2R_W} \frac{\chi_c^g Q}{1 + \chi_c^g} (r - R_{\text{solute}} - R_W) \quad R_{\text{solute}} < r \leq R_{\text{solute}} + R_W \quad (16b)$$

Determination of the Coefficient C in eqs 15 and 16b:

When $r = R_{\text{solute}}$, eq 10a can be written as $P_s^g(R_{\text{solute}}) + \chi_c^g / (2R_W) \int_{R_{\text{solute}}}^{R_{\text{solute}}+R_W} P_s^g(r') dr' = \chi_c^g Q$. Inserting eq 16b into the above equation can determine the coefficient C (see Appendix III) as $C = -(\chi_c^g)^3 Q / [4(1 + \chi_c^g)(2 + \chi_c^g)]$. Hence, replacing C in eqs 15 and 16b yields

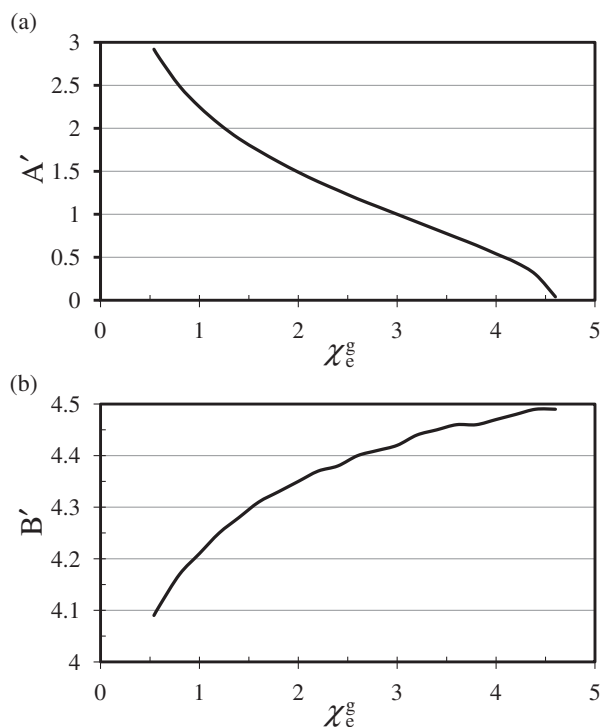


Figure 3. Dependence of the coefficients A' and B' on the χ_c^g . The numerical solutions of (a) A' and (b) B' in eq 14 depend on the solvent molecular electric susceptibility χ_c^g .

respectively. A' and B' were 0.01 between zero and ten steps. Using a given parameter χ_c^g , various values of (A', B') were inserting into the above equation and $J_1(A', B')$ and $J_2(A', B')$ were calculated. Then $(J_1^2 + J_2^2)^{1/2}$ was computed for various values of (A', B') , and the minimum value of $(J_1^2 + J_2^2)^{1/2}$ was picked to examine the proximity to zero.

Results and Discussion

The Oscillation Source of $P_s^g(r)$. The physical meaning of eq 10a can be considered as $P_s^g(r)$ at position r plus the averaged $P_s^g(r)$ over a region multiplied by a constant χ_c^g .

$$P_s^g(r) + \chi_c^g \langle P_s^g(r') \rangle = \chi_c^g Q \quad (18a)$$

$$\langle P_s^g(r') \rangle = \frac{1}{2R_W} \int_{\text{Max}(R_{\text{solute}}, r-R_W)}^{r+R_W} P_s^g(r') dr' = \chi_c^g Q \quad (18b)$$

The $\langle P_s^g(r) \rangle$ is the average $P_s^g(r)$ over a period of $2R_W$.

With $P_s^g(r < R_{\text{solute}}) = 0$, the solution of $P_s^g(r)$ should oscillate in the region $r \geq R_{\text{solute}}$. In far solute regions, $P_s^g(r \rightarrow \infty)$ may approach a constant. The integral region of eq 18b encompasses $(r - R_W)$ to $(r + R_W)$, and the range of integration is $2R_W$. Equation 18 yields an amplitude of $P_s^g(r \rightarrow \infty) = \chi_c^g Q / (1 + \chi_c^g)$. The integral region at the position $r = R_{\text{solute}}$ of eq 18b encompasses R_{solute} to $(R_{\text{solute}} + R_W)$ due to $P_s^g(r < R_{\text{solute}}) = 0$. The integration range is R_W . To satisfy eq 18, the amplitude of $P_s^g(r)$ should be larger than $P_s^g(r \rightarrow \infty)$ near the R_{solute} region. However, the integral region of eq 18b at the position $r = (R_{\text{solute}} + R_W)$ encompasses R_{solute} to $(R_{\text{solute}} + 2R_W)$, and the integration range increases to $2R_W$. To satisfy eq 18, the amplitude of $P_s^g(r)$ has to be less than that of $P_s^g(r \rightarrow \infty)$ near the $(R_{\text{solute}} + R_W)$ region. Hence, the oscillation source of P_s^g comes from the solute excluding solvent molecules leading to $P_s^g(r < R_{\text{solute}}) = 0$, and the solvent molecule at r excluding other solvent molecules leading to eq 18.

Comparison of $P_s^g(r)$ Solved Using eq 10 and $P_s^g(r)$ Computed Using MD Simulations. To understand the performance of eq 10, the solution was verified using a numerical strategy and compared with the solution from MD simulations. The numerical solution from eq 10 oscillates according to the distance to the solute, with a solute molecular radius $R_{\text{solute}} = 2.3 \text{ \AA}$, the solvent molecular radius $R_W = 1.7 \text{ \AA}$, and a solvent molecular electric susceptibility $\chi_c^g = 4.4$, and the oscillation amplitude decays as far away from the solute as observed in MD simulations (Figure 2).

The Amplitude of the First Peak of $P_s^g(r)$ from eq 10 Is Larger than from MD Simulations (Figure 2): The first peak of $g(r)$ is approximately five times higher than the bulk solvent observed in MD simulations,²⁸ but $g(r)$ is 1.0 when deriving eq 10. Hence, the induced solvent dielectric polarization from eq 10 cannot generate an electric field E_{solvent} larger than the electric field from the solute E_{solute} (Figure 1). The net electric field E_{net} from eq 5 is larger than the electric field from MD simulations. Consequently, $p(r)$, which is proportional to E_{net} (eq 2), is larger than the $p(r)$ from MD simulations and $p(r)$ has to be larger to generate enough E_{solvent} to overcome E_{solute} .

The First Valley of $P_s^g(r)$ at $r = 4 \text{ \AA}$ from eq 10 Is Not as Smooth as from MD Simulations (Figure 2): The equation used to calculate the slope of $P_s^g(r)$ is different in the region $r < (R_{\text{solute}} + R_W)$ and $r \geq (R_{\text{solute}} + R_W)$. The cavity radius occupied by solvent molecule is $R_W = 1.7 \text{ \AA}$, and the cavity radius occupied by solute molecule is $R_{\text{solute}} = 2.3 \text{ \AA}$ (Figure 2). Hence, the discontinuous point of differentiation appears at $r = R_{\text{solute}} + R_W = 4.0 \text{ \AA}$.

The Cavity Radius Occupied by Solvent Molecules R_W May Be 1.7 \AA : Several approaches defined the solvent molecular radius, such as that based on a pair distribution function of water oxygen–oxygen, where the position of the first peak is at 2.8 \AA .³³ Hence, the solvent molecular radius is $R_W = 1.4 \text{ \AA}$, and the cavity radius excluding other solvent

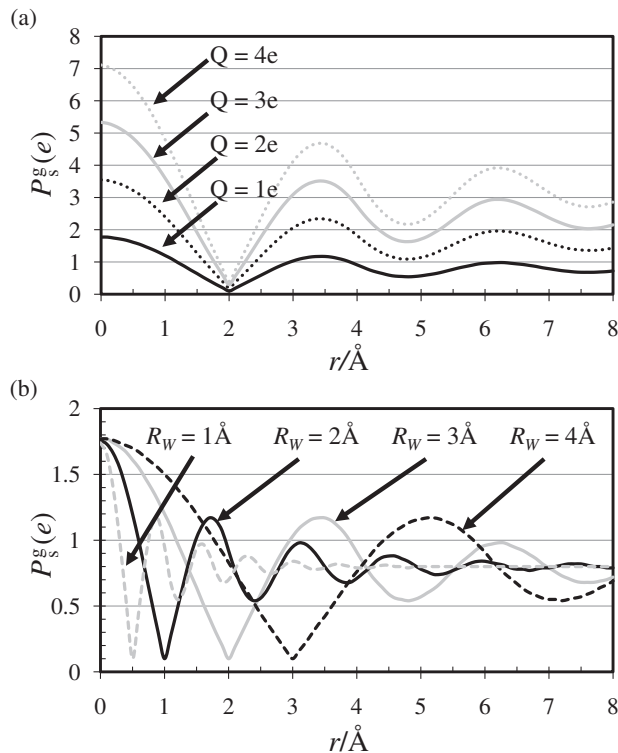


Figure 4. Dependence of the amplitude and period of $P_s^g(r)$ from eq 10 on Q and R_W , respectively. $P_s^g(r)$ as a function of distance r from charged solute atom was computed from eq 10 with numerical strategy with (a) $R_W = 2 \text{ \AA}$, $\chi_c^g = 4$, the solute Q as 1e (solid black), 2e (dashed black), 3e (solid gray), and 4e (dashed gray), respectively. (b) $Q = 1e$, $\chi_c^g = 4$, the solvent molecular radius R_W as 1 (dashed gray), 2 (solid black), 3 (solid gray), and 4 \AA (dashed black), respectively.

molecules is $R_W = 2.8 \text{ \AA}$. Another approach is based on TIP3P force fields,³⁴ where the vdW radius of the TIP3P oxygen atom is $R_{\text{min}}/2 = 1.7682 \text{ \AA}$. In the present paper, the parameter B' in eq 14b is approximately 4.49 when $\chi_c^g = 4.4$ (Figure 3). The period of $P_s^g(r)$ observed in MD simulations (Figure 2) is approximately 2.4 \AA . The period of $P_s^g(r)$ equals $2\pi R_W/B'$ (see “the oscillation period of $P_s^g(r)$ ” paragraph in the theory section). Therefore, the solvent molecular radius is $R_W = 1.7 \text{ \AA}$.

Dependence of the Amplitude and Period of $P_s^g(r)$ from eq 10 on the Solute Charge Q and Solvent Molecular Radius R_W . The numerical solution $P_s^g(r)$ of the integral eq 10 oscillates with decay (Figure 2). The theory section anticipated the amplitude of $P_s^g(r)$ to be proportional to the solute charge Q , which was verified using a numerical solution of eq 10 with various solute charge states Q . Assuming a solvent molecular radius $R_W = 2 \text{ \AA}$, solvent molecular electric susceptibility $\chi_c^g = 4$ and a change from 1e to 4e step 1e in the solute Q results in a $P_s^g(r)$ proportional to the solute charge Q (Figure 4a).

The theory section also anticipated the period of $P_s^g(r)$ to be proportional to the solvent molecular radius R_W . The numerical solution of eq 10 with various solvent molecular radii R_W verified this. When the solute charge $Q = 1e$, the solvent molecular electric susceptibility $\chi_c^g = 4$ and the solvent mo-

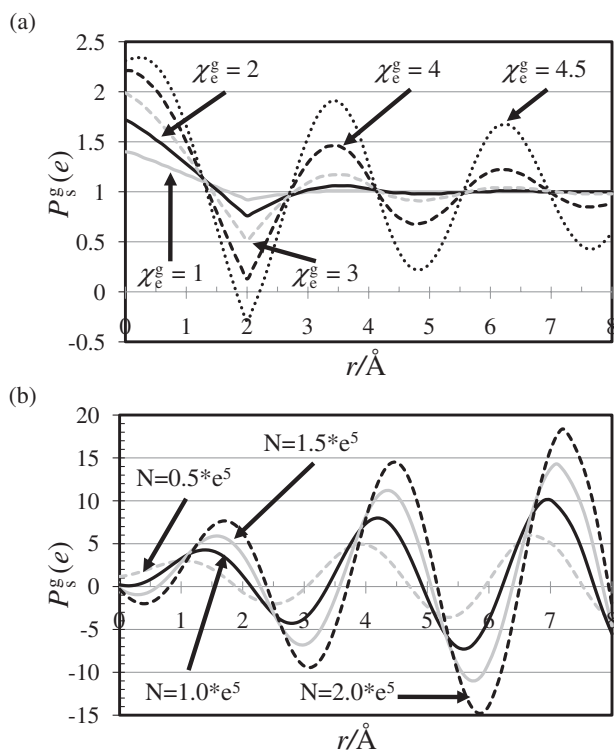


Figure 5. Dependence of the amplitude and period of $P_s^g(r)$ from eq 10 on χ_e^g . $P_s^g(r)$ as a function of distance r from charged solute atom was computed from eq 10 with numerical strategy with (a) $R_W = 2 \text{\AA}$, $Q = (1 + \chi_e^g)/\chi_e^g$, the solvent molecular electric susceptibility $\chi_e^g = 1$ (solid gray), $\chi_e^g = 2$ (solid black), $\chi_e^g = 3$ (dashed gray), $\chi_e^g = 4$ (dashed black), and $\chi_e^g = 4.5$ (dot black). (b) $\chi_e^g = 4.9$, the step numbers of computing are 50000 (dashed gray), 100000 (solid black), 150000 (solid gray), and 200000 (dashed black).

molecular radius R_W changed from 1 to 4 \AA step 1 \AA , then the oscillation period was proportional to the solvent molecular radius R_W (Figure 4b).

Dependence of $P_s^g(r)$ from eq 10 on χ_e^g . The dependence of $P_s^g(r)$ from eq 10 on the solvent molecular electric susceptibility χ_e^g was explored using a numerical strategy. $P_s^g(r)$ oscillation decays according to the distance to the solute when the solvent molecular electric susceptibility $\chi_e^g \leq 4.5$ (Figure 5a), but the peak of the amplitude of $P_s^g(r)$ increases with the distance to the solute when the solvent molecular electric susceptibility $\chi_e^g \geq 4.9$ (Figure 5b). Although the amplitudes of the oscillation peak and valley depend on the solvent molecular electric susceptibility χ_e^g , the positions of the oscillation peak and valley are independent of the solvent molecular electric susceptibility χ_e^g .

When the solvent molecular electric susceptibility $\chi_e^g = 1$ or 2, the amplitude of the oscillation peak is not large and the oscillation peak disappears quickly. When the solvent molecular electric susceptibility χ_e^g approaches 4.7–4.8, the oscillation peak decays slowly (Figure 5a). For $\chi_e^g \geq 4.9$, the oscillation peak increases (Figure 5b). With more numerical iterations for solving $P_s^g(r)$ in eq 10, the amplitude of $P_s^g(r)$ increases and the convergent curve of $P_s^g(r)$ cannot be found (Figure 5b).

When $\chi_e^g \leq 4.5$, the oscillation peak increases and its rate accelerates as the solvent molecular electric susceptibility χ_e^g increases (Figure 5a). If χ_e^g appeared only in the right side of eq 10 as the solute charge Q , the amplitude of $P_s^g(r)$ would be proportional to χ_e^g , because the amplitude of $P_s^g(r)$ is proportional to the solute charge Q . However, the solvent molecular electric susceptibility χ_e^g also appears in the second term of eq 10. Thus, the rate of the oscillation amplitude increases when the solvent molecular electric susceptibility χ_e^g increases and the oscillation amplitude increases according to the distance to the solute when $\chi_e^g > 4.9$.

Dependence of the Coefficients A and B on R_W and χ_e^g . The coefficients A and B depend on the solvent molecular radius R_W and solvent molecular electric susceptibility χ_e^g , and are required for computing $P_s^g(r)$ in eq 17. The coefficients A and B can be calculated from A' and B' based on the relation $A' = AR_W$ and $B' = BR_W$. The coefficients A' and B' depend on the solvent molecular electric susceptibility χ_e^g and a numerical strategy using various values of χ_e^g can solve A' and B' . When χ_e^g increases from 0.54 to 4.5, the coefficient A' decreases from 2.93 to 0.04 (Figure 3a), while the coefficient B' increases from 4.09 to 4.49 (Figure 3b). For $\chi_e^g \leq 0.54$ or $\chi_e^g \geq 4.6$, a numerical solution for A' and B' cannot be found.

The Performance of the Approximate Analytical Solution for $P_s^g(r)$ from eq 17. To derive an analytical solution of eq 17 from eq 10, an approximate strategy was applied. To examine the performance of the derived analytical solution for $P_s^g(r)$, $P_s^g(r)$ from eq 17 was compared with the numerical solution from eq 10 using various solute charge states Q , solvent molecular radii R_W and solvent molecular electric susceptibility χ_e^g . The results demonstrated that the curve of the proposed approximate analytical solution from eq 17 is similar to the numerical solution in eq 10 (Figure 6).

An inconsistency occurs in the region $r \leq R_{\text{solute}} + R_W$, where the linear approximation in eq 17 differs from the curve derived from the numerical solution of eq 10 (Figure 6). Equation 16a yields a more accurate analytical solution for $P_s^g(r)$ in the region $r \leq R_{\text{solute}} + R_W$. To simplify the analytical solution describing $P_s^g(r)$ in the region $r \leq R_{\text{solute}} + R_W$, eq 16b uses a linear curve to replace the curve in eq 16a. Hence, the analytical solution of eq 17 in the region $r \leq R_{\text{solute}} + R_W$ is linear, which is slightly different from the numerical solution of eq 10.

Comparison of the Equations Describing Oscillation Decay and Harmonic Damping. The numerical solution for $P_s^g(r)$ from eq 10 oscillates with decay according to the distance to solute, and is consistent with the proposed analytical solution for $P_s^g(r)$ in eq 17. The format of the proposed analytical solution in eq 17 oscillates with an exponential decay similar to the format of the solution from a harmonic damping system, such as a spring system or RLC (R: resistor, L: inductor, C: capacitor) electric circuits. However, the format of eq 10 differs from harmonic damping (Table 1).

For example, the spring system may consider a particle with mass m attached to a spring. The force from the spring will push back to the equilibrium state as $-kx$ following Hooke's law.³⁵ The force from the spring equals the mass times acceleration ma or $m\partial^2x/\partial t^2$. The friction force is proportional to the velocity, $f\partial x/\partial t$. The equation of the spring system is

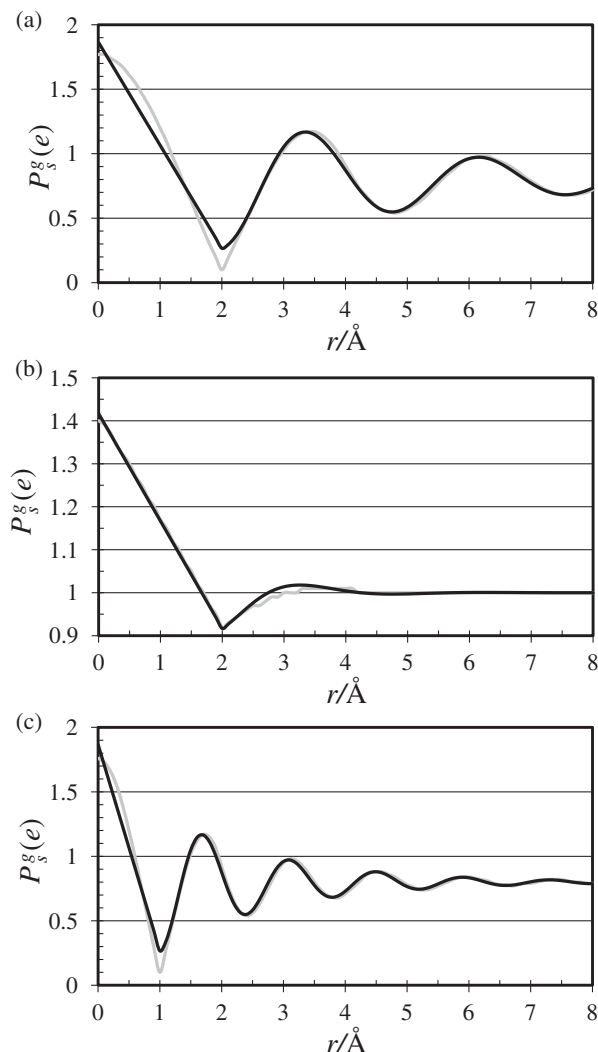


Figure 6. Comparison of $P_s^g(r)$ computed from eqs 17 and 10. $P_s^g(r)$ as a function of distance r from charged solute atom was computed from eq 17 (black curve) and eq 10 with numerical strategy (gray curve) respectively. The curves of $P_s^g(r)$ related to r are plotted with the set of (Q, R_W, χ_e^g) parameters which are (a) $(Q = 1e, R_W = 2 \text{ \AA}, \text{ and } \chi_e^g = 4)$, (b) $(Q = 2e, R_W = 2 \text{ \AA}, \text{ and } \chi_e^g = 1)$, and (c) $(Q = 1e, R_W = 1 \text{ \AA}, \text{ and } \chi_e^g = 4)$.

$$m \frac{d^2x}{dt^2} + f \frac{dx}{dt} + kx = 0 \quad (19)$$

Assuming that the solution of eq 19 is harmonic damping, then

$$x(t) = x(0)e^{-at} \cos(bt) \quad (20)$$

where $x(0)$ is the initial position of the particle with mass m . The damping factor a and the oscillation frequency b depend on the mass m , the friction coefficient f , and the spring constant k (Appendix V). Thus,

$$\begin{cases} a = f/(2m) \\ b = (f^2 - 4maf + 4mk)^{1/2}/(2m) \approx \sqrt{k/m} \end{cases} \quad (21)$$

The solution format of harmonic damping (eq 20) from eq 19 is similar to the distance-dependent oscillating decay solution (eq 15) from eq 10. In most cases, the oscillation solution comes from the second-order differential equation as in eq 19, because a second-order differential of the sin or cosine function will return to a sin or cosine function. In contrast, eq 10a is a first-order integral equation. A mass-spring system generates oscillation, because the initial position of the particle in the spring system is not in the equilibrium position. The spring force repeats a pattern of pulling particles back and then over the equilibrium position. The near-solute solvent polarization oscillates, because $P_s^g(r) = 0$ in the region $r < R_{\text{solute}}$ and because $P_s^g(r)$ has to satisfy the condition, $P_s^g(r) + \chi_e^g \langle P_s^g(r) \rangle = \text{constant}$ (eq 18a). The damping phenomenon of eq 19 derives from the friction coefficient. The amplitude peak of $P_s^g(r)$ decays due to the solvent molecular electric susceptibility χ_e^g .

Conclusion

An approximate equation describing $P_s^g(r)$ is derived for spherical solutes. The numerical solution of eq 10 is similar to the solution from MD simulations and can reproduce oscillating decay characteristics of $P_s^g(r)$. $P_s^g(r)$ oscillates near the solute region, because $P_s^g(r)$ is zero in the solute occupied region, and the condition for $P_s^g(r) + \chi_e^g \langle P_s^g(r) \rangle$ being a constant is satisfied. The solvent molecular electric susceptibility χ_e^g determines the peak amplitude of the oscillation of $P_s^g(r)$ and the decay rate of the oscillation peak of $P_s^g(r)$ according to the distance to the solute. If χ_e^g is greater than 4.9, the amplitude of the oscillation peak of $P_s^g(r)$ may increase in mathematical solutions. Furthermore, the size of solvent molecules determines the oscillation period of $P_s^g(r)$, and the amplitude of

Table 1. Comparison of the Equations Where Oscillation Damping Solutions Can Be Generated

	Equation derived in this project	Harmonic damping
Equation	$P_s^g(r) + \frac{\chi_e^g}{2R_W} \int_{\text{Max}(R_{\text{solute}}, r-R_W)}^{r+R_W} P_s^g(r') dr' = \chi_e^g Q$ (eq 10a)	$m \frac{d^2x}{dt^2} + f \frac{dx}{dt} + kx = 0$ (eq 19)
Boundary/initial condition	$P_s^g(r) = 0$ for $r < R_{\text{solute}}$	$x = x(0)$
Solution	$P_s^g(r) = \frac{\chi_e^g Q}{1 + \chi_e^g} + Ce^{-A(r-R_{\text{solute}}-R_W)} \cos(B(r-R_{\text{solute}}-R_W))$ (eq 15)	$x(t) = x(0)e^{-at} \cos(bt)$ (eq 20)
Damping/oscillation factors	$\begin{cases} AR_W = -\chi_e^g \sinh AR_W \cos BR_W \\ BR_W = -\chi_e^g \cos AR_W \sin BR_W \end{cases}$ (eq 14)	$\begin{cases} a = f/(2m) \\ b \approx \sqrt{k/m} \end{cases}$ (eq 21)

$P_s^g(r)$ is proportional to the charged state of the solute. The approximate analytical solution of $P_s^g(r)$ is based on the analyzed results and agrees well with the numerical solution of $P_s^g(r)$. The oscillation decay solution is similar to the harmonic damping solution, but has a different equation format.

Appendix

Derivation of eq 14a. In the region $r \geq (R_{\text{solute}} + R_W)$, $y_h(r)$ should satisfy the derived differential equation as follows:

$$\frac{dy_h(r)}{dr} = -\frac{\chi_c^g}{2R_W} [y_h(r + R_W) - y_h(r - R_W)] \quad r \geq R_{\text{solute}} + R_W \quad (12)$$

The proposed homogeneous solution y_h is described as follows:

$$y_h(r) = Ce^{-A(r-R_{\text{solute}}-R_W)} \cos(B(r-R_{\text{solute}}-R_W)) \quad x \geq R_{\text{solute}} + R_W \quad (13)$$

By substituting $y_h(r)$ in eq 13 into $y_h(r)$ in eq 12, $dy_h(r)/dr$, $y_h(r + R_W)$ and $y_h(r - R_W)$ in the region $r \geq (R_{\text{solute}} + R_W)$ can then be computed as follows, respectively:

$$\begin{aligned} \frac{dy_h(r)}{dr} &= -Ce^{-A(r-R_{\text{solute}}-R_W)} \left[\begin{array}{l} A \cos(B(r-R_{\text{solute}}-R_W)) \\ + B \sin(B(r-R_{\text{solute}}-R_W)) \end{array} \right] \\ &= -Ce^{-A(r-R_{\text{solute}}-R_W)} \left[\begin{array}{l} A \cos(BR_W) \cos(B(r-R_{\text{solute}})) \\ + A \sin(BR_W) \sin(B(r-R_{\text{solute}})) \\ + B \cos(BR_W) \sin(B(r-R_{\text{solute}})) \\ - B \sin(BR_W) \cos(B(r-R_{\text{solute}})) \end{array} \right] \end{aligned} \quad (I.1)$$

$$y_h(r + R_W) = Ce^{-A(r-R_{\text{solute}})} \cos(B(r-R_{\text{solute}})) \quad (I.2)$$

$$\begin{aligned} y_h(r - R_W) &= Ce^{-A(r-R_{\text{solute}}-2R_W)} \cos(B(r-R_{\text{solute}}-2R_W)) \\ &= Ce^{-A(r-R_{\text{solute}}-2R_W)} \left[\begin{array}{l} \cos(2BR_W) \cos(B(r-R_{\text{solute}})) \\ + \sin(2BR_W) \sin(B(r-R_{\text{solute}})) \end{array} \right] \end{aligned} \quad (I.3)$$

It follows by substituting eqs I.1, I.2, and I.3 into eq 12 that

$$\begin{aligned} &-Ce^{-A(r-R_{\text{solute}}-R_W)} \left[\begin{array}{l} A \cos(BR_W) \cos(B(r-R_{\text{solute}})) \\ + A \sin(BR_W) \sin(B(r-R_{\text{solute}})) \\ + B \cos(BR_W) \sin(B(r-R_{\text{solute}})) \\ - B \sin(BR_W) \cos(B(r-R_{\text{solute}})) \end{array} \right] \\ &= -\frac{\chi_c^g}{2R_W} \left\{ \begin{array}{l} Ce^{-A(r-R_{\text{solute}})} \cos(B(r-R_{\text{solute}})) \\ - Ce^{-A(r-R_{\text{solute}}-2R_W)} \left[\begin{array}{l} \cos(2BR_W) \cos(B(r-R_{\text{solute}})) \\ + \sin(2BR_W) \sin(B(r-R_{\text{solute}})) \end{array} \right] \end{array} \right\} \end{aligned} \quad (I.4)$$

After decomposing eq I.4 based on the function containing $\cos(B(r-R_{\text{solute}}))$ and $\sin(B(r-R_{\text{solute}}))$ components, eq I.4 can be written as follows:

$$\begin{aligned} &-Ce^{-A(r-R_{\text{solute}}-R_W)} \left[\begin{array}{l} A \cos(BR_W) \cos(B(r-R_{\text{solute}})) \\ - B \sin(BR_W) \cos(B(r-R_{\text{solute}})) \end{array} \right] \\ &= -\frac{\chi_c^g}{2R_W} \left\{ \begin{array}{l} Ce^{-A(r-R_{\text{solute}})} \cos(B(r-R_{\text{solute}})) \\ - Ce^{-A(r-R_{\text{solute}}-2R_W)} [\cos(2BR_W) \cos(B(r-R_{\text{solute}}))] \end{array} \right\} \end{aligned} \quad (I.5a)$$

$$\begin{aligned} &-Ce^{-A(r-R_{\text{solute}}-R_W)} \left[\begin{array}{l} A \sin(BR_W) \sin(B(r-R_{\text{solute}})) \\ + B \cos(BR_W) \sin(B(r-R_{\text{solute}})) \end{array} \right] \\ &= -\frac{\chi_c^g}{2R_W} \{-Ce^{-A(r-R_{\text{solute}}-2R_W)} [\sin(2BR_W) \sin(B(r-R_{\text{solute}}))]\} \end{aligned} \quad (I.5b)$$

Equation I.5 can be organized as follows:

$$\begin{cases} A \cos(BR_W) - B \sin(BR_W) = \frac{\chi_c^g}{2R_W} [e^{-AR_W} - e^{AR_W} \cos(2BR_W)] \\ A \sin(BR_W) + B \cos(BR_W) = -\frac{\chi_c^g}{R_W} \sin(2BR_W) \end{cases} \quad (I.6)$$

Equation I.6 can be written in the matrix format:

$$\begin{bmatrix} \cos(BR_W) & -\sin(BR_W) \\ \sin(BR_W) & \cos(BR_W) \end{bmatrix} \begin{bmatrix} A \\ B \end{bmatrix} = \frac{\chi_c^g}{2R_W} \begin{bmatrix} e^{-AR_W} - e^{AR_W} \cos(2BR_W) \\ -e^{AR_W} \sin(2BR_W) \end{bmatrix} \quad (I.7)$$

The constants A and B can be found as follows:

$$\begin{aligned} \begin{bmatrix} A \\ B \end{bmatrix} &= \frac{\chi_c^g}{2R_W} \begin{bmatrix} \cos(BR_W) & -\sin(BR_W) \\ \sin(BR_W) & \cos(BR_W) \end{bmatrix}^{-1} \begin{bmatrix} e^{-AR_W} - e^{AR_W} \cos(2BR_W) \\ -e^{AR_W} \sin(2BR_W) \end{bmatrix} \\ &= \frac{\chi_c^g}{2R_W} \begin{bmatrix} \cos(BR_W) & \sin(BR_W) \\ -\sin(BR_W) & \cos(BR_W) \end{bmatrix} \begin{bmatrix} e^{-AR_W} - e^{AR_W} \cos(2BR_W) \\ -e^{AR_W} \sin(2BR_W) \end{bmatrix} \\ &= \frac{\chi_c^g}{2R_W} \begin{bmatrix} e^{-AR_W} \cos(BR_W) - e^{AR_W} \cos(BR_W) \cos(2BR_W) - e^{AR_W} \sin(BR_W) \sin(2BR_W) \\ -e^{-AR_W} \sin(BR_W) + e^{AR_W} \sin(BR_W) \cos(2BR_W) - e^{AR_W} \cos(BR_W) \sin(2BR_W) \end{bmatrix} \end{aligned} \quad (I.8)$$

It follows by substituting $\cos 2BR_W = 2 \cos^2 BR_W - 1$ and $\sin 2BR_W = 2 \sin BR_W \cos BR_W$ into eq I.8 that

$$\begin{aligned} \begin{bmatrix} A \\ B \end{bmatrix} &= \frac{\chi_c^g}{2R_W} \begin{bmatrix} e^{-AR_W} \cos(BR_W) - e^{AR_W} \cos(BR_W)(2 \cos^2(BR_W) - 1) - 2e^{AR_W} \sin^2(BR_W) \cos(BR_W) \\ -e^{-AR_W} \sin(BR_W) + e^{AR_W} \sin(BR_W)(2 \cos^2(BR_W) - 1) - 2e^{AR_W} \sin(BR_W) \cos^2(BR_W) \end{bmatrix} \\ &= \frac{\chi_c^g}{2R_W} \begin{bmatrix} e^{-AR_W} \cos(BR_W) - 2e^{AR_W} \cos^3(BR_W) + e^{AR_W} \cos(BR_W) - 2e^{AR_W} \sin^2(BR_W) \cos(BR_W) \\ -e^{-AR_W} \sin(BR_W) + 2e^{AR_W} \sin(BR_W) \cos^2(BR_W) - e^{AR_W} \sin(BR_W) - 2e^{AR_W} \sin(BR_W) \cos^2(BR_W) \end{bmatrix} \\ &= \frac{\chi_c^g}{2R_W} \begin{bmatrix} e^{-AR_W} \cos(BR_W) - e^{AR_W} \cos(BR_W) \\ -e^{-AR_W} \sin(BR_W) - e^{AR_W} \sin(BR_W) \end{bmatrix} \end{aligned} \quad (I.9)$$

The solutions for A and B can be organized as follows:

$$\begin{cases} A = -\frac{\chi_c^g}{R_W} \sinh(AR_W) \cos(BR_W) \\ B = -\frac{\chi_c^g}{R_W} \cosh(AR_W) \sin(BR_W) \end{cases} \quad (I.10)$$

Derivation of eq 16a. In the region $r \leq R_{\text{solute}} + R_W$, $P_s^g(r)$ satisfies the condition in eq 10b.

$$\frac{dP_s^g(r)}{dr} = -\frac{\chi_c^g}{2R_W} P_s^g(r + R_W) \quad (10b)$$

From eq 10b, $dP_s^g(r)/dr$ in the region $R_{\text{solute}} < r \leq R_{\text{solute}} + R_W$ is dependent on $P_s^g(r)$ in the region $R_{\text{solute}} + R_W < r \leq R_{\text{solute}} + 2R_W$.

In the region $r \geq (R_{\text{solute}} + R_W)$, the solution for $P_s^g(r)$ is proposed in eq 15:

$$P_s^g(r) = \frac{\chi_c^g Q}{1 + \chi_c^g} + C e^{-A(r - R_{\text{solute}} - R_W)} \cos(B(r - R_{\text{solute}} - R_W)) \quad r \geq R_{\text{solute}} + R_W \quad (15)$$

By substituting $P_s^g(r)$ in eq 15 into the right side of eq 10b, $dP_s^g(r)/dr$ in the region $R_{\text{solute}} < r \leq R_{\text{solute}} + R_W$ can be written as

$$\frac{dP_s^g(r)}{dr} = -\frac{\chi_c^g}{2R_W} \left[\frac{\chi_c^g Q}{1 + \chi_c^g} + C e^{-A(r - R_{\text{solute}})} \cos(B(r - R_{\text{solute}})) \right] \quad (II.1)$$

It follows with the formulas from the integral table that

$$\int e^{-Ax} \cos(Bx) dx = \frac{e^{-Ax}}{A^2 + B^2} [B \sin(Bx) - A \cos(Bx)] \quad (II.2)$$

Also, $P_s^g(r)$ can be evaluated by integration of $dP_s^g(r)/dr$ over r , i.e.,

$$\begin{aligned} P_s^g(r) &= -\frac{\chi_c^g}{2R_W} \frac{\chi_c^g Q}{1 + \chi_c^g} r \\ &\quad - C \frac{\chi_c^g}{2R_W} \frac{e^{-A(r - R_{\text{solute}})}}{A^2 + B^2} [B \sin(B(r - R_{\text{solute}})) \\ &\quad - A \cos(B(r - R_{\text{solute}}))] + D \end{aligned} \quad (II.3)$$

where D is a constant.

To keep continuity at the point $r = R_{\text{solute}} + R_W$, replace r by $R_{\text{solute}} + R_W$ in eq 15 as follows:

$$P_s^g(R_{\text{solute}} + R_W) = \frac{\chi_c^g Q}{1 + \chi_c^g} + C \quad (II.4)$$

Also replace r by $R_{\text{solute}} + R_W$ in eq II.3 as follows:

$$\begin{aligned} P_s^g(R_{\text{solute}} + R_W) &= -\frac{\chi_c^g}{2R_W} \frac{\chi_c^g Q}{1 + \chi_c^g} (R_{\text{solute}} + R_W) \\ &\quad - C \frac{\chi_c^g}{2R_W} \frac{e^{-AR_W}}{A^2 + B^2} [B \sin(BR_W) \\ &\quad - A \cos(BR_W)] + D \end{aligned} \quad (II.5)$$

The coefficient D in eq II.3 can be evaluated by equivalent eqs II.4 and II.5 as follows:

$$\begin{aligned} D &= \frac{\chi_c^g Q}{1 + \chi_c^g} + C + \frac{\chi_c^g}{2R_W} \frac{\chi_c^g Q}{1 + \chi_c^g} (R_{\text{solute}} + R_W) \\ &\quad + C \frac{\chi_c^g}{2R_W} \frac{e^{-AR_W}}{A^2 + B^2} [B \sin(BR_W) - A \cos(BR_W)] \end{aligned} \quad (II.6)$$

Substituting the coefficient D into eq II.3, then the solution $P_s^g(r)$ in the region $R_{\text{solute}} < r \leq R_{\text{solute}} + R_W$ can be written as follows:

$$\begin{aligned} P_s^g(r) &= -\frac{\chi_c^g}{2R_W} \frac{\chi_c^g Q}{1 + \chi_c^g} r \\ &\quad - C \frac{\chi_c^g}{2R_W} \frac{e^{-A(r - R_{\text{solute}})}}{A^2 + B^2} [B \sin(B(r - R_{\text{solute}})) \\ &\quad - A \cos(B(r - R_{\text{solute}}))] \\ &\quad + \frac{\chi_c^g Q}{1 + \chi_c^g} + C + \frac{\chi_c^g}{2R_W} \frac{\chi_c^g Q}{1 + \chi_c^g} (R_{\text{solute}} + R_W) \\ &\quad + C \frac{\chi_c^g}{2R_W} \frac{e^{-AR_W}}{A^2 + B^2} [B \sin(BR_W) - A \cos(BR_W)] \end{aligned} \quad (II.7)$$

Equation II.7 can then be reorganized as follows:

$$\begin{aligned} P_s^g(r) &= \frac{\chi_c^g Q}{1 + \chi_c^g} + C \\ &\quad + C \frac{\chi_c^g}{2R_W} \frac{e^{-AR_W}}{A^2 + B^2} [B \sin(BR_W) - A \cos(BR_W)] \end{aligned}$$

$$\begin{aligned}
& -\frac{\chi_c^g}{2R_W} \frac{\chi_c^g Q}{1+\chi_c^g} (r - R_{\text{solute}} - R_W) \\
& -C \frac{\chi_c^g}{2R_W} \frac{e^{-A(r-R_{\text{solute}})}}{A^2+B^2} [B \sin(B(r-R_{\text{solute}}))] \\
& -A \cos(B(r-R_{\text{solute}}))]
\end{aligned} \quad (\text{II.8})$$

Determine the Coefficient C in eqs 15 and 16b. The solution of $P_s^g(r)$ in the region $R_{\text{solute}} < r \leq R_{\text{solute}} + R_W$ is approximated as

$$P_s^g(r) \approx \frac{\chi_c^g Q}{1+\chi_c^g} + C - \frac{\chi_c^g}{2R_W} \frac{\chi_c^g Q}{1+\chi_c^g} (r - R_{\text{solute}} - R_W) \quad (\text{16b})$$

When $r = R_{\text{solute}}$, eq 16b can be written as below:

$$P_s^g(R_{\text{solute}}) \approx \frac{\chi_c^g Q}{1+\chi_c^g} + C + \frac{\chi_c^g}{2} \frac{\chi_c^g Q}{1+\chi_c^g} \quad (\text{III.1})$$

The relation between $P_s^g(r)$ and solute charge Q can be approximated as

$$P_s^g(r) + \frac{\chi_c^g}{2R_W} \int_{\text{Max}(R_{\text{solute}}, r-R_W)}^{r+R_W} P_s^g(r') dr' = \chi_c^g Q \quad (\text{10a})$$

When $r = R_{\text{solute}}$, eq 10a can be written as below:

$$P_s^g(R_{\text{solute}}) + \frac{\chi_c^g}{2R_W} \int_{R_{\text{solute}}}^{R_{\text{solute}}+R_W} P_s^g(r') dr' = \chi_c^g Q \quad (\text{III.2})$$

The second term of eq III.2 can be obtained by integrating $P_s^g(r)$ over r' , i.e.,

$$\begin{aligned}
\int_{R_{\text{solute}}}^{R_{\text{solute}}+R_W} P_s^g(r') dr' &= \int_{R_{\text{solute}}}^{R_{\text{solute}}+R_W} \left[\frac{\chi_c^g Q}{1+\chi_c^g} + C - \frac{\chi_c^g}{2R_W} \frac{\chi_c^g Q}{1+\chi_c^g} (r' - R_{\text{solute}} - R_W) \right] dr' \\
&= R_W \left[\frac{\chi_c^g Q}{1+\chi_c^g} + C - \frac{\chi_c^g}{2R_W} \frac{\chi_c^g Q}{1+\chi_c^g} (-R_{\text{solute}} - R_W) \right] \\
&\quad - \frac{\chi_c^g}{2R_W} \frac{\chi_c^g Q}{1+\chi_c^g} \frac{(R_{\text{solute}} + R_W)^2 - R_{\text{solute}}^2}{2} \\
&= R_W \left[\frac{\chi_c^g Q}{1+\chi_c^g} + C + \frac{\chi_c^g}{2R_W} \frac{\chi_c^g Q}{1+\chi_c^g} (R_{\text{solute}} + R_W) \right] \\
&\quad - \frac{\chi_c^g}{2R_W} \frac{\chi_c^g Q}{1+\chi_c^g} \frac{2R_{\text{solute}}R_W + R_W^2}{2} \\
&= \frac{R_W \chi_c^g Q}{1+\chi_c^g} + CR_W + \frac{\chi_c^g}{2} \frac{\chi_c^g Q R_{\text{solute}}}{1+\chi_c^g} + \frac{\chi_c^g}{2} \frac{\chi_c^g Q R_W}{1+\chi_c^g} \\
&\quad - \frac{\chi_c^g}{2} \frac{\chi_c^g Q R_{\text{solute}}}{1+\chi_c^g} - \frac{\chi_c^g}{2} \frac{\chi_c^g Q R_W}{1+\chi_c^g} \\
&= \frac{R_W \chi_c^g Q}{1+\chi_c^g} + CR_W + \frac{\chi_c^g}{4} \frac{\chi_c^g Q R_W}{1+\chi_c^g}
\end{aligned} \quad (\text{III.3})$$

It follows by substituting eqs III.1 and III.3 into eq III.2 that

$$\begin{aligned}
& \left(\frac{\chi_c^g Q}{1+\chi_c^g} + C + \frac{\chi_c^g}{2} \frac{\chi_c^g Q}{1+\chi_c^g} \right) + \frac{\chi_c^g}{2R_W} \left(\frac{R_W \chi_c^g Q}{1+\chi_c^g} + CR_W + \frac{\chi_c^g}{4} \frac{\chi_c^g Q R_W}{1+\chi_c^g} \right) = \chi_c^g Q \\
& \frac{\chi_c^g Q}{1+\chi_c^g} + C + \frac{\chi_c^g}{2} \frac{\chi_c^g Q}{1+\chi_c^g} + \frac{\chi_c^g}{2} \frac{\chi_c^g Q}{1+\chi_c^g} + \frac{\chi_c^g}{2} C + \frac{\chi_c^g}{2} \frac{\chi_c^g}{4} \frac{\chi_c^g Q}{1+\chi_c^g} = \chi_c^g Q \\
& C + \frac{\chi_c^g}{2} C = \chi_c^g Q - \frac{\chi_c^g Q}{1+\chi_c^g} - \chi_c^g \frac{\chi_c^g Q}{1+\chi_c^g} - \frac{\chi_c^g}{2} \frac{\chi_c^g}{4} \frac{\chi_c^g Q}{1+\chi_c^g} \\
& \left(1 + \frac{\chi_c^g}{2} \right) C = -\frac{(\chi_c^g)^2}{8} \frac{\chi_c^g Q}{1+\chi_c^g} \\
& \frac{(2+\chi_c^g)}{2} C = -\frac{(\chi_c^g)^2}{8} \frac{\chi_c^g Q}{1+\chi_c^g} \\
& C = -\frac{(\chi_c^g)^2}{4} \frac{\chi_c^g Q}{(1+\chi_c^g)(2+\chi_c^g)}
\end{aligned} \quad (\text{III.4})$$

Derivation the Period of Oscillation $P_s^g(r)$ in eq 17. From eq 17, $P_s^g(r)$ in the region $r \geq (R_{\text{solute}} + R_W)$ is

$$P_s^g(r) = \frac{\chi_c^g Q}{1+\chi_c^g} - \frac{(\chi_c^g)^2}{4} \frac{\chi_c^g Q}{(1+\chi_c^g)(2+\chi_c^g)} e^{-A(r-R_{\text{solute}}-R_W)} \cos(B(r-R_{\text{solute}}-R_W)) \quad (\text{17})$$

The differential of $P_s^g(r)$ over r is

$$\frac{dP_s^g(r)}{dr} = \frac{(\chi_c^g)^2}{4} \frac{\chi_c^g Q}{(1+\chi_c^g)(2+\chi_c^g)} \left[A e^{-A(r-R_{\text{solute}}-R_W)} \cos(B(r-R_{\text{solute}}-R_W)) + B e^{-A(r-R_{\text{solute}}-R_W)} \sin(B(r-R_{\text{solute}}-R_W)) \right] \quad (\text{IV.1})$$

To satisfy the condition $dP_s^g(r)/dr = 0$, the following condition can be obtained.

$$A \cos(B(r - R_{\text{solute}} - R_{\text{W}})) + B \sin(B(r - R_{\text{solute}} - R_{\text{W}})) = 0 \quad (\text{IV.2})$$

And then,

$$\tan(B(r - R_{\text{solute}} - R_{\text{W}})) = -\frac{A}{B} \quad (\text{IV.3})$$

$$r = R_{\text{solute}} + R_{\text{W}} + \frac{1}{B} \left(\pi - \tan^{-1} \left(\frac{A}{B} \right) \right) \quad (\text{IV.4})$$

Hence, the period of $P_{\text{S}}^{\text{g}}(r)$ in the region $r \geq (R_{\text{solute}} + R_{\text{W}})$ is $2\pi/B$.

Derivation of eq 21. Take the spring system as an example. Consider a particle with mass m attached to a spring. The force from the spring will push back to the equilibrium state following Hooke's law as $-kx$. The force from the spring equals the mass times the acceleration ma , or $m\partial^2 x/\partial t^2$. And the friction force is proportional to the velocity, $f\partial x/\partial t$. The equation of the spring system can be written as

$$m \frac{d^2 x}{dt^2} + f \frac{dx}{dt} + kx = 0 \quad (19)$$

Assume the solution of eq 19 is harmonic damping, i.e.,

$$x(t) = x(0)e^{-at} \cos(bt) \quad (20)$$

The first-order differential equation of $x(t)$ is

$$\frac{dx}{dt} = -ae^{-at} \cos(bt) - be^{-at} \sin(bt) \quad (\text{V.1})$$

The second-order differential equation of $x(t)$ is

$$\frac{d^2 x}{dt^2} = (a^2 - b^2)e^{-at} \cos(bt) + 2abe^{-at} \sin(bt) \quad (\text{V.2})$$

Substituting eqs 20, V.1, and V.2 into eq 19, we obtain that

$$m(a^2 - b^2)e^{-at} \cos(bt) + 2mabe^{-at} \sin(bt) - afe^{-at} \cos(bt) - bfe^{-at} \sin(bt) + ke^{-at} \cos(bt) = 0 \quad (\text{V.3})$$

The coefficients of $\sin(bt)$ and $\cos(bt)$ terms in eq V.3 should be zero, respectively.

$$\begin{cases} m(a^2 - b^2) - af + k = 0 \\ 2mab - bf = 0 \end{cases} \quad (\text{V.4})$$

It follows from eq V.4 that

$$a = f/2m \quad (\text{V.5})$$

and then

$$b = \left[\frac{f^2 - 4maf + 4mk}{4m^2} \right]^{1/2} \approx \sqrt{\frac{k}{m}} \quad (\text{V.6})$$

We thank Professor Martin Karplus for the CHARMM program. This work was supported by the Institute of Biomedical Sciences, Academia Sinica, the Grants NSC 97-2218-E-214-008-MY3 from the National Science Council of Taiwan, ISU 97-S-10 and ISU 98-S-06 from I-SHOU University of Taiwan.

References

- 1 D. J. Griffiths, *Introduction to Electrodynamics*, 3rd ed., Prentice Hall, Upper Saddle River, NJ, **1999**.
- 2 J. D. Jackson, *Classical Electrodynamics*, 3rd ed., John Wiley & Sons, New York, **1999**.
- 3 B. Lewin, *Genes VIII*, Pearson Prentice Hall, Upper Saddle River, NJ, **2004**.
- 4 A. L. Lehninger, D. L. Nelson, M. M. Cox, *Principles of Biochemistry: With an Extended Discussion of Oxygen-Binding Proteins*, 2nd ed., Worth Publishers, New York, **1993**.
- 5 J. M. Berg, J. L. Tymoczko, L. Stryer, *Biochemistry*, 6th ed., W. H. Freeman, New York, **2006**.
- 6 B. G. Maiya, T. Ramasarma, *Curr. Sci.* **2001**, 80, 1523.
- 7 P. Ball, *Chem. Rev.* **2008**, 108, 74.
- 8 M. Feig, A. Onufriev, M. S. Lee, W. Im, D. A. Case, C. L. Brooks, III, *J. Comput. Chem.* **2004**, 25, 265.
- 9 J. Wagoner, N. A. Baker, *J. Comput. Chem.* **2004**, 25, 1623.
- 10 J. Tomasi, *Theor. Chem. Acc.* **2004**, 112, 184.
- 11 J. Tomasi, B. Mennucci, R. Cammi, *Chem. Rev.* **2005**, 105, 2999.
- 12 J. Tomasi, M. Persico, *Chem. Rev.* **1994**, 94, 2027.
- 13 A. Morreale, R. Gil-Redondo, A. R. Ortiz, *Proteins* **2007**, 67, 606.
- 14 T. Wang, R. C. Wade, *Proteins* **2003**, 50, 158.
- 15 B. K. Shoichet, A. R. Leach, I. D. Kuntz, *Proteins* **1999**, 34, 4.
- 16 M. Born, *Z. Phys.* **1920**, 1, 45.
- 17 S. A. Adcock, J. A. McCammon, *Chem. Rev.* **2006**, 106, 1589.
- 18 K. Binder, J. Horbach, W. Kob, W. Paul, F. Varnik, *J. Phys.: Condens. Matter* **2004**, 16, S429.
- 19 G. Ciccotti, D. Frenkel, I. R. McDonald, *Simulation of Liquids and Solids: Molecular Dynamics and Monte Carlo Methods in Statistical Mechanics*, North-Holland, Amsterdam, **1987**.
- 20 B. J. Sung, A. Yethiraj, *J. Chem. Phys.* **2003**, 119, 6916.
- 21 H.-J. Woo, A. R. Dinner, B. Roux, *J. Chem. Phys.* **2004**, 121, 6392.
- 22 M. P. Taylor, J. E. G. Lipson, *J. Chem. Phys.* **1998**, 109, 7583.
- 23 S. Ten-no, S. Iwata, *J. Chem. Phys.* **1999**, 111, 4865.
- 24 Q. Du, D. Beglov, B. Roux, *J. Phys. Chem. B* **2000**, 104, 796.
- 25 M. N. Lotfollahi, H. Modarress, *J. Chem. Phys.* **2002**, 116, 2487.
- 26 T. Imai, A. Kovalenko, F. Hirata, *Chem. Phys. Lett.* **2004**, 395, 1.
- 27 R. Zhou, G. Krilov, B. J. Berne, *J. Phys. Chem. B* **2004**, 108, 7528.
- 28 P.-K. Yang, C. Lim, *J. Comput. Chem.* **2009**, 30, 700.
- 29 A. K. Soper, *Chem. Phys.* **2000**, 258, 121.
- 30 A. P. Lyubartsev, A. Laaksonen, *Phys. Rev. E: Stat. Phys., Plasmas, Fluids, Relat. Interdiscip. Top.* **1995**, 52, 3730.
- 31 P.-K. Yang, C. Lim, *J. Phys. Chem. B* **2008**, 112, 10791.
- 32 P.-K. Yang, C. Lim, *J. Phys. Chem. B* **2008**, 112, 14863.
- 33 A. H. Narten, W. E. Thiessen, L. Blum, *Science* **1982**, 217, 1033.
- 34 W. L. Jorgensen, J. Chandrasekhar, J. D. Madura, R. W. Impey, M. L. Klein, *J. Chem. Phys.* **1983**, 79, 926.
- 35 D. Halliday, R. Resnick, J. Walker, *Fundamentals of Physics*, 7th ed., John Wiley & Sons, New York, **2004**.